11th International Symposium on Magnetic Bearings
August 26-29, Nara, Japan

MODELING AND CONTROL OF AN AXIAL MAGNETIC BEARING FOR A PROTOTYPE OF ELECTRIC MOTOR SUPPORTED BY RADIAL MAGNETIC BEARINGS

Vagner P. das Neves
Brazilian Navy
vagnerdasneves@hotmail.com
José Andrés Santisteban
Electrical Engineering Dept., PGMEC, Fluminense Federal University
Niterói, RJ, 24210-240, Brazil
jasantisteban@vm.uff.br
André Plaisant
Electrical Engineering Dept., Fluminense Federal University
Niterói, RJ, 24210-240, Brazil
plaisant@vm.uff.br

ABSTRACT
Research on magnetic bearings is being conducted in universities and research centers all over the world. Among the main advantages of the use of these devices are the reduction of friction losses and their corresponding necessity for maintenance. Magnetic bearings can already be found in rotating machines in medical, food, oil, and military industries. As to electric machines, the use of such electromagnets provides a natural instability to the system. Therefore, controllers become necessary to hold the rotor in an equilibrium position, without contact with the stator. In this work, modeling, implementation, and practical results of an axial position controller is presented. An axial controller has been designed to be implemented on an experimental prototype that consists of an induction motor, arranged in the horizontal position, already supported by radially controlled magnetic bearings. Different from other approaches, the experimental stiffness and damping observed along the axial direction, when only the radial magnetic bearings are acting, was taken into account for the controller design.

INTRODUCTION
Traditionally, rotors of electrical machines rest on ball bearings or sliding bearings (oil lubricated). These mechanical devices supply radial and axial forces allowing the rotor axis stay stationary respect to the stator. The so called magnetic bearings, on the other hand, use electromagnetic forces to support a rotor, eliminating the mechanical contact between the rotor and the stator and so the friction losses. When the magnetic fields are generated through windings, they are named active magnetic bearings (AMB) because their currents are appropriately controlled using the principles of feedback control. Additionally, depending on the mechanical type of load, these can be classified as radial AMB or axial AMB.

Due to their operative characteristics, some interesting advantages can also be mentioned: automatic balance, vibration control, and, as a consequence, the extended life of the machines. The magnetic bearings are promising in several industrial segments, such as food, medical, aeronautics, vehicular, space, nuclear energy, oil and chemistries in general [1], [2].

In Brazil, some researches on magnetic bearings and bearingless motors are also being reported. In particular, the split-winding stator approach [3] was proposed more than two decades ago. In this work, on the other hand, the authors refer to a prototype of an induction motor, horizontally supported by conventional AMB, which has been continuously investigated [4], [5], [6], [7]. On these approaches, the axial control of the rotor has been usually considered as a decoupled issue from the radial control [8], [9], however, experimental results have shown that axial forces generated by radial magnetic bearings should be considered. With this in mind, a second-order mechanical model for the axial direction is proposed based on experimental tests. In this approach, equivalent stiffness and damping were taken into account in the controller design which, implemented with analogic circuits, is operating satisfactorily.

Prototype Description

The electric motor under study consists of a commercially-available 2hp, 2-pole, three-phase, cage induction type, which had its original stator and rotor characteristics preserved [4], [5]. Their end covers were substituted by new ones where the additional stators, of radial and axial AMB´s, were mounted. Fig. 1 shows the actual view of this prototype and Fig. 2 shows the

details of the complete shaft, holding the motor rotor and the four rotors of the AMB´s. In the center of this figure, a little cap, which holds the speed sensor, is shown. In the upper left part, one can see the 8-pole radial AMB stator and the circular axial AMB stator. Four inductive sensors were installed in each cover of the motor.

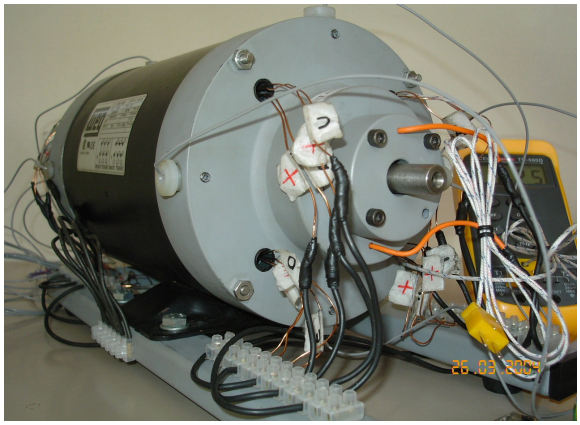

FIGURE 1: View of the motor prototype with AMB´s.

THE PLANT MODELLING

As mentioned, the prototype was already functioning with the two radial AMB´s. The corresponding control was implemented by means of a personal computer and A/D and D/A cards. In this condition, it was confirmed that the shaft had an auto-positioning behavior, in such a way that the magnetic fluxes would find the lowest reluctance path along their trajectory. This behavior had not been initially considered when the axial magnetic bearings were designed [4]. In the present work, the initially disregarded coupling between radial and axial directions is taken into account in the design of the axial controller.

With this in mind, in order to obtain an appropriated model of the mechanical system in the axial direction, it has been proposed an experiment which consists in manually displacing the shaft until one of its maximum axial positions and, then, releasing it all of a sudden. The acquired signal of the position sensor represents the homogeneous response of the mechanical system with the initial condition $x=0.00035m$, as shown in Fig. 3.

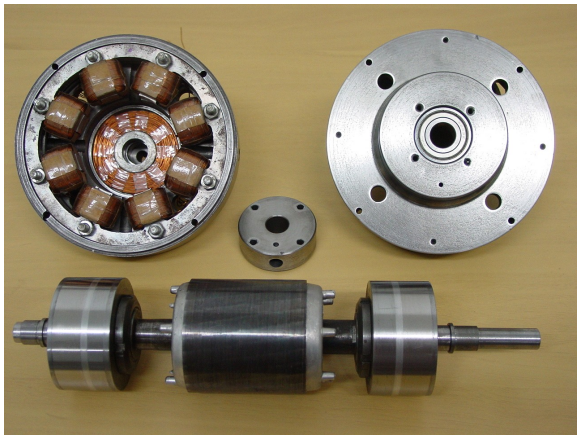

FIGURE 2: Main internal parts of the prototype.

The oscillating dynamic characteristic of the horizontal position suggests, as a first approximation, an under-damped second-order function. The analysis of this response, at the light of the second-order systems performance parameters, took us to a transfer function of a controller aiming the damping of perturbations on the axial positioning of the shaft. The simplified axial-direction mechanical system model has been represented through components which are proportional to the horizontal displacement, velocity, and acceleration:

$$F = m \cdot \ddot{x} + k_v \cdot \dot{x} + k_x \cdot x, \qquad (1)$$

where m is the mass of the shaft and all the rotors, K_v, the velocity proportionality constant, and K_x, the displacement proportionality constant.

The parameters of the canonic expression for a second-order system transfer function [10] have been obtained directly from Fig. 3:

$$G(s) = \frac{\omega_n^2}{s^2 + 2 \cdot \zeta \cdot \omega_n \cdot s + \omega_n^2}, \qquad (2)$$

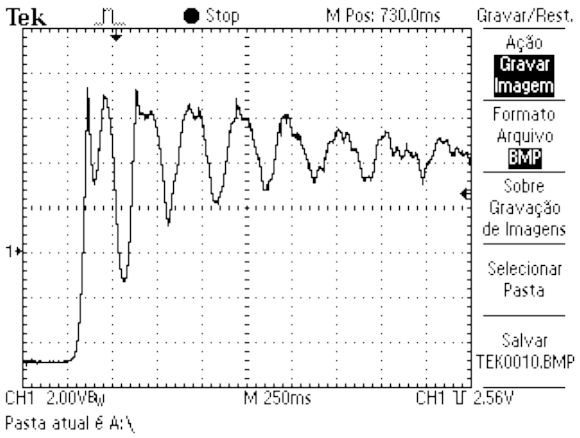

FIGURE 3: Natural response of the shaft position after having released it from $x = 0.00035m$ (Vert: 0.2 mm/div, Hor:250 ms/div).

where ω_n is the undamped natural frequency, and ξ, the damping coefficient.

The coefficients of the characteristic polynomial meet their physical counterparts as:

$$\frac{k_v}{m} = 2 \cdot \zeta \cdot \omega_n \qquad \frac{k_x}{m} = \omega_n^2$$

Still, the relationship between the *2%* settling time and the decaying rate σ is given by:

$$t_a = 4 \cdot T = \frac{4}{\sigma} = \frac{4}{\zeta \cdot \omega_n}.$$

From the homogeneous response, the undamped natural frequency has been determined to be $\omega_n = 22,8$ *rad/s* ; and the settling time $t_s = 1,5s$. Using the mass value as $m = 5,3042$ *kg,* we have reached to:

$$K_v = 28,29 \; kg/s,$$
$$K_x = 2.795,05 \; N/m.$$

Considering all the values obtained so far, the transfer function that models this axial mechanical characteristic of the motor becomes

$$G(s) = \frac{0.1885}{s^2 + 5.3335 \cdot s + 526.95}. \qquad (3)$$

As to validate the transfer function above, it has been simulated on the graphic environment *Simulink*, of the Matlab dynamic digital simulation application. Figs. 4 and 5 show the theoretical realization diagram of this plant subsystem and its step response respectively.

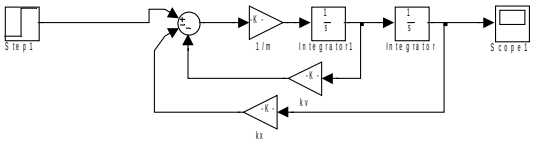

FIGURE 4: Realization diagram of the mechanical subsystem.

Now, in order to complete the modeling of the plant representing the axial magnetic bearing, the relationship between the force exerted by the magnetic fields and the currents that create them has been considered. Fig. 6 depicts a schematic diagram of the split actuator of the axial magnetic bearings which exposes its differential nature [1].

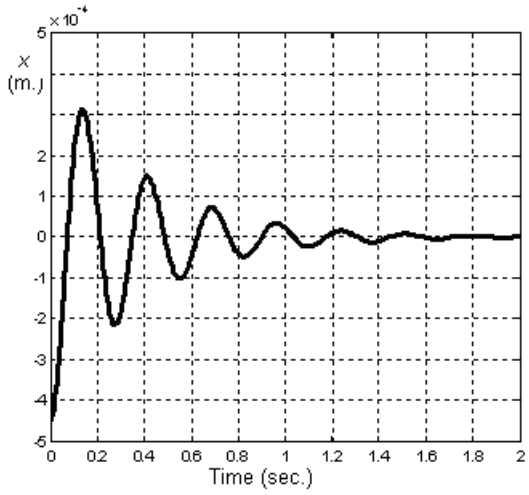

FIGURE 5: Theoretical homogeneous response of the mechanical subsystem.

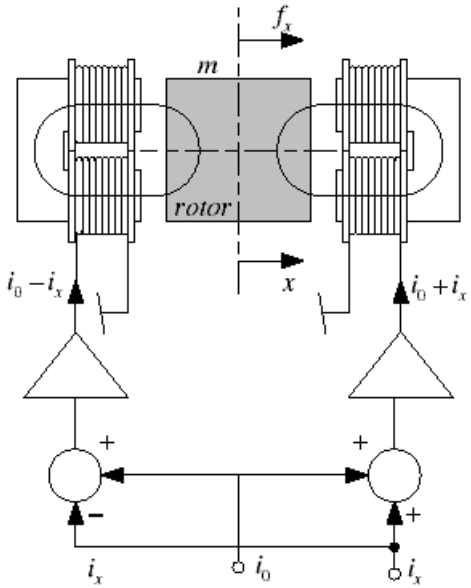

FIGURE 6: Axial magnetic bearings acting in differential mode.

The difference between the forces acting on the rotor is given by

$$f_x = f_+ - f_- = k \cdot \left[\frac{(i_o + i_x)^2}{(s_o - x)^2} - \frac{(i_o - i_x)^2}{(s_o + x)^2} \right], \qquad (4)$$

where:

$$k = \frac{1}{4} \cdot \mu_o \cdot n^2 \cdot A_0,$$

Considering the application of this relationship to the present work, n is the number of turns of one of the axial magnetic bearing windings, A_0 is the transversal area of the iron core, μ_o is the magnetic field constant of the air, x is the axial displacement of the shaft in relation to the equilibrium point, s_0 is the air gap distance which defines the equilibrium point ($0.45mm$), i_x is the control current, and i_o is the bias current.

Taking into account that $x << s_0$, this relation can be linearized, obtaining:

$$f_x = \frac{4 \cdot k \cdot i_o}{s_o^2} \cdot i_x + \frac{4 \cdot k \cdot i_o^2}{s_o^3} \cdot x = k_i \cdot i_x + k_s \cdot x \qquad (5)$$

Fig. 7 presents the dimensions of the implemented stator for both axial magnetic bearings. Now, considering $n=150$ as the number of turns, and $\mu_o=4\pi \cdot 10^{-7}$ Vs/Am as the magnetic permeability, one can obtain $k=3,9725 \cdot 10^{-6}$.

Making use of k, and taking into account the bias current $i_o=1,3A$, leads to $k_i=101,368$ and $k_s=2,2526 \cdot 10^5$. In this way, the following expression (6) is formed, which can be represented in a block diagram as in fig. 8.

$$X(s) = \left(\frac{\mathbf{0.1885}}{s^2 + \mathbf{5.3335} \cdot s + \mathbf{526.95}} \cdot \right) [k_i \cdot I_x(s) + k_s \cdot X(s)] \qquad (6)$$

The closed-loop transfer function of the above system is given by:

$$\frac{X(s)}{I_x(s)} = \frac{\mathbf{101.368}}{\mathbf{5.3042} \cdot s^2 + \mathbf{28.29} \cdot s - \mathbf{2.224} \cdot \mathbf{10^5}} \qquad (7)$$

THE CONTROLLER DESIGN

The dynamics of the system to be controlled has required a compensator with an anticipatory characteristic, so that it allowed a fast control action. Such a controller has been implemented as a combination of proportional and derivative components in parallel (PD) [10].

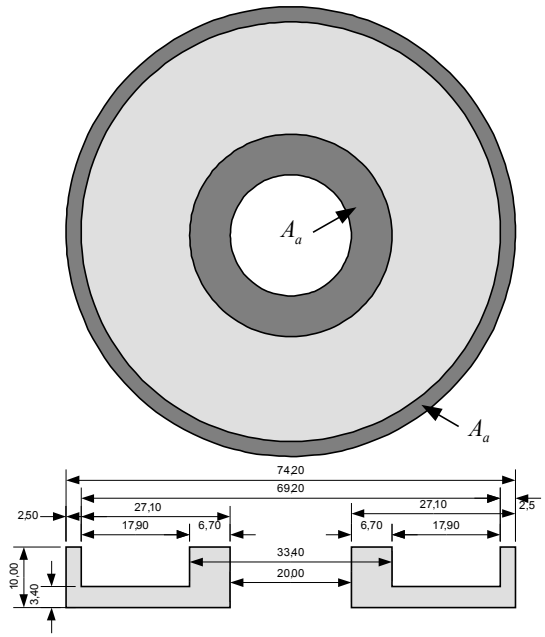

FIGURE 7: Axial magnetic bearing dimensions (mm).

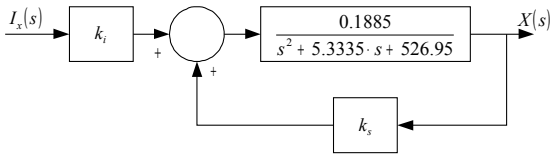

FIGURE 8: Block diagram of the linearized model.

Determination of Parameters.

The starting point has been the desired approximate settling time $t_s= 0.025s$, and a damping coefficient $\xi =0.76$. These choices resulted in undamped natural and damped frequencies $\omega_n=210,5263$ rad/s, and $\omega_d=136,8259$ rad/s, respectively.

These values define the desirable dominant poles as $p = \sigma \pm j\omega_d = - 160,000 \pm j\ 210,5263$. The angle criterion (Fig. 9) determines that a PD controller should contribute with an supplementary angle to the one shown in Eq. (8). Such effect has been obtained with a zero at $s=-355,46$, providing the angle $\alpha =47^o$.

$$\angle \left. \frac{1.01 \cdot 10^2}{5.30 \cdot s^2 + 28.29 \cdot s - 2.22 \cdot 10^5} \right|_{s=-1.60 \cdot 10^2 \pm j \cdot 2.11 \cdot 10^2} \cong -227.12^\circ \qquad (8)$$

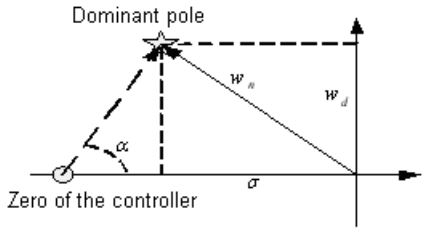

FIGURE 9: The dominant pole, the zero of the controller and the angle α.

The choice of a gain $K_C=700$ defines the controller transfer function as $C(s)=700(s+355,46)$, and provides the system with a *2%* settling time of approximately *0,016s*.

The resulting block diagram of the controlled system is presented in fig. 10, from which the corresponding open-loop transfer function (9) and root locus can be obtained (Fig. 11).

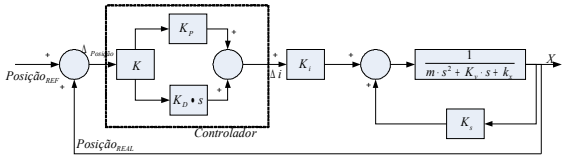

FIGURE 10: Block diagram of the controlled system.

$$G = 133.7763 \cdot \frac{(s + 355.4600)}{s^2 + 5.3335 \cdot s - 4.1910 \cdot 10^4} \qquad (9)$$

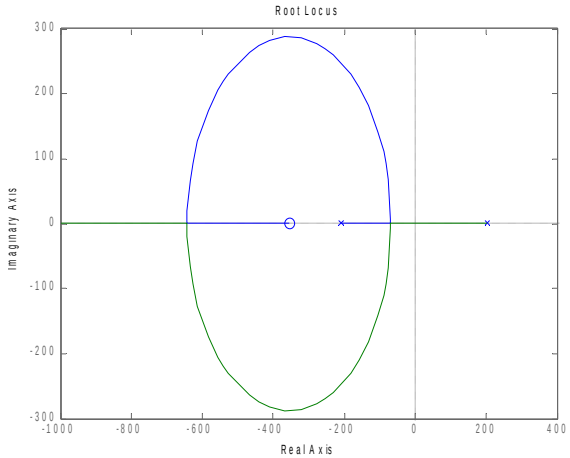

FIGURE 11: Root locus of the controlled system.

Fig. 12 shows the schematic electronic circuits, with operational amplifiers, on which has been based the physical implementation. The proportional control actions have been realized with input and feedback resistors $R_i=100\ \Omega$ and $R_f=118\ \Omega$, respectively, for the series gain, and $R_{Pi}=28,5\ k\Omega$ and $R_{Pf}=1k\Omega$, respectively, for the parallel gain.

For the derivative control action, a feedback resistor $R_{f2}=11k\Omega$, and an input capacitor $C_{Di}=15\ \mu F$, increased by a noise filter, supplied by the feedback capacitor $C_{Df}=1\ \eta F$ have been used.

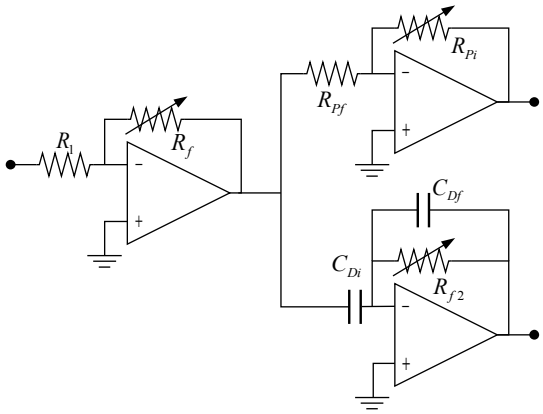

FIGURE 12: PD controller with noise filter.

EXPERIMENTAL RESULTS

Based on the model obtained, and recalling the usual modeling of magnetic forces in axial magnetic bearings [1], the analog control has been implemented and connected to the motor.

Fig. 13 shows a reference step and the corresponding response at the axial position of the rotor. Although the intention of the axial control is to reject perturbations, this test illustrates the efficiency of the designed controller. In this figure, the bias current I_{or} of the radial magnetic bearing was set at 0.39A.

In order to show the influence of the radial magnetic bearings on the axial direction, some tests were made for two different values of $I_{or:}$ 0.39A and 0.975A. Figs. 14 and 15 show axial reference steps from 0mm to -0.1mm and back to 0mm, and from 0mm to +0.1mm and back to 0 mm.

These results suggest that a change on the bias current of the radial magnetic bearings should imply a corresponding adjustment on the mechanical model of the axial direction and on the parameters of the controller in order to obtain a similar performance.

CONCLUSIONS

An improved modeling for the axial behavior of a rotor supported by radial magnetic bearings, having in mind the application of axial magnetic bearings, was realized. A second-order approximate model was derived from an experimental test. It was confirmed that the equivalent stiffness and damping depend on the bias currents of the pre-existent radial magnetic bearings. A simple analog circuit was designed and tested to control the axial displacement of the rotor. Successful experimental results confirm the validity of this approach.

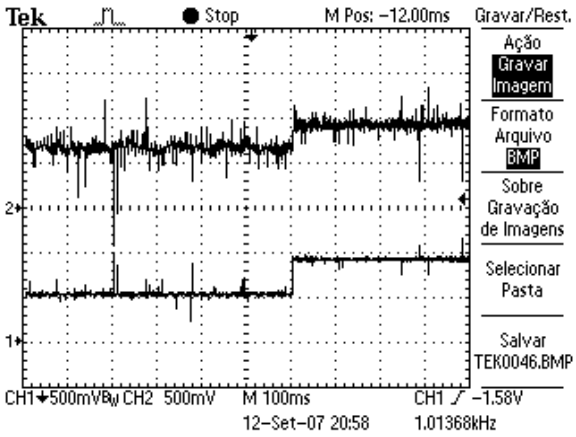

FIGURE 13: Reference step from 0,055mm to 0,090mm (Ch. 1), and output (Ch. 2) (Ver: 0,05mm/V, Hor:100ms/div).

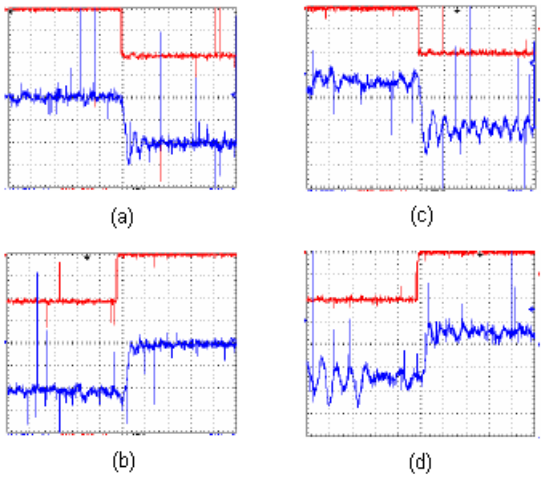

FIGURE 14: Responses (lower traces) to reference steps (upper traces):
(a) 0mm to -0.10mm with I_{or} = 0.39A
(b) -0.1mm. to 0mm. with I_{or} = 0.39A
(c) 0mm to -0.10mm with I_{or} = 0.975A
(d) -0.1mm. to 0mm. with I_{or} = 0.975A
(Ver: 0,05mm/div, Hor: 25ms/div).

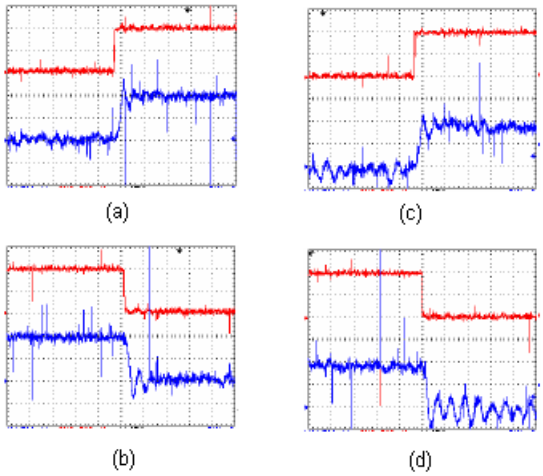

FIGURE 15: Responses (lower traces) to reference steps (upper traces):
(a) 0mm to +0.10mm with I_{or} = 0.39A
(b) +0.1mm. to 0mm. with I_{or} = 0.39A
(c) 0mm to +0.10mm with I_{or} = 0.975A
(d) +0.1mm. to 0mm. with I_{or} = 0.975A
(Ver: 0,05mm/div, Hor: 25ms/div).

ACKNOWLEDGMENT

The authors would like to thank the Brazilian research council (Conselho Nacional de Pesquisa - CNPq) for having supported this work.

REFERENCES

1. Schweitzer, G.; Bleuler, H. and Traxler, A. Active magnetic bearings. vdf Hochschul-verlag AG na der ETH Zürich, Switzerland, 240p,1994.
2. Chiba, A.; Fukao, T.; Ichikawa, O.; Oshima, M.; Takemoto, M. and Dorrell, D. G., Magnetic Bearings and Bearingless Drives. Newness, Elsevier, 381 p.,2005.
3. Salazar, A. O., Chiba A., Fukao T., A Review of Developments in Bearingless Motors, Seventh International Symposium on Magnetic Bearings, pp. 335, Zürich, Aug, 2000.
4. Chapetta, R. A.; Santisteban J. A. e Noronha, R. F. (2002). Mancais Magnéticos - Uma Metodologia de Projeto. In: Congresso Nacional de Engenharia Elétrica - CONEM 2002, João Pessoa. Anais do II Congresso Nacional de Engenharia Mecânica, 2002.
5. Santisteban J. A.; Noronha, R. F.; David, D. e Pedrosa, J. F. Dimensionamento Mecânico, Fabricação e Montagem de um Protótipo de Motor Elétrico Suportado por Mancais Magnéticos. In: III Congresso Nacional de Engenharia Mecânica. CONEM 2004, Belém, Pará, 2004.

6. Velandia, E. F. R.; Santisteban, J. A.; Noronha, R. F. and Silva, V. A. P. Development of a Magnetically borne Electrical motor prototype. Proceedings of COBEM 2005. 18th International Congress of Mechanical Engineering, Ouro Preto, Minas Gerais, Brazil, November 6-11, 2005.
7. Rodrigues, A. R. L. e Santisteban, J. A. . Projeto e Simulação de Controladores de Posição para um Motor Elétrico Suportado por Mancais Magnéticos. Revista Pesquisa Naval, Brasília, No 19. p. 9-15, 2006.
8. Santisteban J. A. and Méndes, S. R., Fuzzy Control of an Axial Magnetic Bearing. In: The 16th International Conference on Magnetically Levitated Systems and Linear Drives, 2000. Proceedings of the MAGLEV'2000, Rio de Janeiro. p. 207-212, 2000.
9. Santisteban J. A.; Méndes, S. R. and Sacramento, D. S., Design and Implementation of a Fuzzy Controller for an Axial Magnetic Bearing .ISIE '03. IEEE International Symposium on Industrial Electronics, p. 991- 994, vol.2., 2003.
10. Ogata, K., Engenharia de Controle Moderno. 4a Edição. Rio de Janeiro: Prentice-Hall do Brasil, 700p., 2003.